

Nanoscale

Accepted Manuscript



This is an *Accepted Manuscript*, which has been through the Royal Society of Chemistry peer review process and has been accepted for publication.

Accepted Manuscripts are published online shortly after acceptance, before technical editing, formatting and proof reading. Using this free service, authors can make their results available to the community, in citable form, before we publish the edited article. We will replace this *Accepted Manuscript* with the edited and formatted *Advance Article* as soon as it is available.

You can find more information about *Accepted Manuscripts* in the [Information for Authors](#).

Please note that technical editing may introduce minor changes to the text and/or graphics, which may alter content. The journal's standard [Terms & Conditions](#) and the [Ethical guidelines](#) still apply. In no event shall the Royal Society of Chemistry be held responsible for any errors or omissions in this *Accepted Manuscript* or any consequences arising from the use of any information it contains.

ARTICLE

Operating principles of in-plane silicon nanowires at simple step-edges

Cite this: DOI: 10.1039/x0xx00000x

Mingkun Xu^{a,c}, Zhaoguo Xue^a, Linwei Yu^{a,b*}, Shengyi Qian^a, Zheng Fan^b, Junzhuan Wang^a, Jun Xu^a, Yi Shi^a, Kunji Chen^a and Pere Roca i Cabarrocas^b

Received 00th January 2012,

Accepted 00th January 2012

DOI: 10.1039/x0xx00000x

www.rsc.org/

Growing silicon nanowires (SiNWs) into precise locations is a key enabling technology for SiNWs-based device applications. This can be achieved via an in-plane growth of SiNWs along a simple step-edge, where metal catalyst droplets absorb amorphous Si matrix to produce c-SiNWs. However, a comprehensive understanding of this phenomenon is still lacking. We here establish an analytic model to address the driving force that dictates the growth dynamics under various droplet-step contact configurations, and to identify the key control parameters for effective guided growth. These new principles are verified against a series of experimental observations and prove to be powerful in designing a stable guided growth configuration. Furthermore, we propose and demonstrate a unique ability to achieve in-situ capturing, guiding and releasing of the in-plane SiNWs along curved step-edges. We suggest that these new understanding and results could also provide a fundamental basis and practical guide for positioning and integrating self-assembled nanowires in a wide variety of material systems.

Introduction

Self-assembly growth mediated by nanoscale metal catalyst droplets enable a low-cost and high throughput production of silicon nanowires (SiNWs), which are essential building blocks to a wide variety of nanoelectronics and optoelectronic applications¹⁻³. To integrate the SiNWs functionalities, growing SiNWs into precise locations is crucial³⁻⁹. So far, most of the self-assembly SiNWs have been grown via a vapor-liquid-solid (VLS) process where the precursors are gaseous silane^{5, 10-14}. To align and position such VLS-grown SiNWs, one has to use pre-defined alumina nano porous membrane^{9, 15}, electro-beam lithography defined guiding channels⁶ or sophisticated post-growth manipulations⁵, which are by themselves complicated fabrication procedures or involve costly nano-operations. Another interesting strategy to enable a lateral growth of VLS-grown GaAs nanowires has been proposed by Fortuna and Zhang, where an epitaxial interface formed between the GaAs nanowires upon GaAs (100) substrate can help to guide in-plane GaAs nanowires into specific crystallographic orientation^{16, 17}.

Recently, we discovered that a thin film of hydrogenated amorphous Si (a-Si:H) deposited on substrate surface can be adopted as a solid precursor medium, which enables us to confine naturally the growth of SiNWs into an in-plane or on-surface mode, mediated by *surface-running* indium catalyst droplets¹⁸⁻²⁰. During such an in-plane solid-liquid-solid (IPSLS) growth, the catalyst droplets absorb Si atoms from a-Si:H matrix, where the Si atoms see a higher Gibbs energy than that in c-Si, and deposit crystalline SiNW behind^{19, 21-23}. An unique opportunity of the IPSLS-growth lies that, the liquid catalyst

droplet moving among *rigid* a-Si:H precursor layer (in strong contrast to the *soft* gaseous environment in VLS growth) is very sensitive to local surface patterns or even slight relief variations. This feature can help to dictate the growth course of the in-plane SiNWs^{19, 21, 22} by defining very simple and convenient surface patterns that require no high resolution lithography. Indeed, we have observed experimentally that the catalyst droplet can be directed by an etched SiNx step-edge to produce in-plane SiNWs exactly along the guiding edge^{20, 24}. However, understanding of this guided growth phenomenon remains still empirical²⁴. A comprehensive model of this guiding growth in general, or the extent to which this strategy is applicable in specific, has to be established to provide a more reliable guideline for future device applications. The purpose of this work is thus to address first the critical fundamental aspects of the guided growth behavior, taking place at a simple step-edge, and then we will examine these growth control principles against direct experimental observations, and explore them to demonstrate a series of interesting in-situ operations of the in-plane SiNWs by curved step-edge.

Experiments

The guiding step-edges were fabricated by etching into a pre-coated SiN_x layer (~180 nm thick) on top of Si wafer or Corning substrates, joining ITO stripe lines at the crossings as illustrated in Fig. 1a and 1b. Then, the substrates were loaded into a conventional plasma enhanced chemical vapour deposition (PECVD) system. By H₂ plasma treatment at 250°C, the exposed ITO pads are superficially reduced to precipitate indium (In) nano-droplets, then the surface was coated with a-Si:H layer (of nominal thickness from 10 nm to 30 nm) at a

lower substrate temperature of around 100°C, as depicted in Fig. 1c. The growth of in-plane SiNWs was activated when the substrate was heated again to 450°C and kept in vacuum for 1 hour. During this annealing step, the In catalyst drops start to move around by absorbing Si atoms from the front a-Si:H matrix and producing crystalline SiNWs behind. More discussion and experimental details are available in our previous reports^{19, 21, 22}.

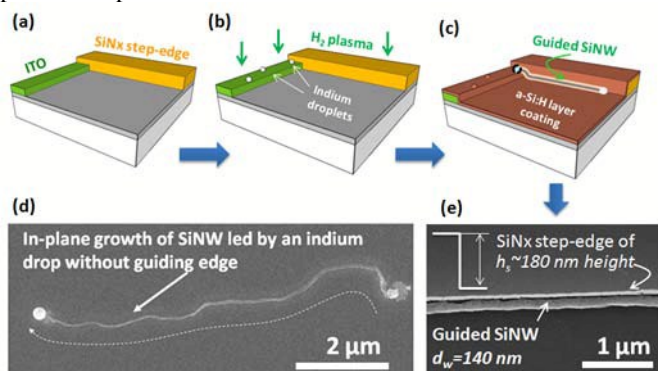


Fig. 1: (a)-(c) illustrate the fabricate steps for step guided growth of in-plane silicon nanowires (SiNWs); (d) presents the SEM image of the growth of a single free SiNW without guiding step-edge, while (e) shows a guided in-plane SiNW along SiNx step edge of ~ 180nm high.

Formulation and Discussion

During the in-plane growth, the SiNWs are produced continuously along the moving course of the leading catalyst droplets, for example the one produced by a catalyst droplet free-roaming on planar surface, seen in the SEM image in Fig. 1d. To control the growth course, a simple step-edge can be defined to *influence* the movement of the catalyst droplet, as witnessed in Fig. 1e, where an in-plane SiNW of 140 nm in diameter has been guided to grow along the step-edge. As we know, the growth of in-plane SiNWs is directed by the surface running In catalyst droplets. It is the movement of the catalyst droplet that has to be precisely controlled in order to guide and position the in-plane SiNWs into the right places. To achieve that, we rely on a unique feature of the in-plane growth of SiNW that can help to drive the liquid catalyst droplet into pre-designed moving course, that is, during the IPSLS growth, the catalyst droplets are sandwiched by a front absorption interface between a-Si:H/catalyst droplet and a rear deposition interface catalyst droplet/SiNW. Both of them are *hard* liquid-solid interfaces, which is in strong contrast to the *soft* gaseous environment in a VLS process. In order to keep a balance growth rate of the front and the rear interfaces, as formulated in more details later, the liquid In droplet will be forced to deform from a sphere shape (which is energetically favourable with a minimum surface Gibbs energy of G_{min}). This deformation or geometric distortion can be quantified by an extra Gibbs surface energy (δG) compared to that of a spherical one. Usually, the release of such extra Gibbs surface energy will cause rich growth dynamics, including regular switching of growth direction or sidewall corrugation of the in-plane SiNWs, as reported in our previous works^{22, 25}. Here we focus on an important fact that the introduction of a step-edge, which are also coated with a uniform layer of a-Si:H on both the planar and sidewall surfaces, will alter the local growth balance condition for the catalyst droplet, or in other words, this will

modify the extra Gibbs surface energy profile seen by a moving catalyst droplet. This differentiated energy profile can thus drive the catalyst droplet to follow or be repelled from the step-edge under different contacting configurations, and thus control the position and alignment of the produced in-plane SiNWs.

To formulate this extra Gibbs surface energy under specific growth condition, we first consider a spherical catalyst drop with an initial diameter of d_c being placed upon a planar or *flat* substrate surface covered by an a-Si:H layer of h_a thick. When the temperature is raised, the catalyst drop becomes molten and absorbs the a-Si:H coating layer to form initial c-Si nucleation seed within the catalyst droplet. Then, it kicks off the lateral movement by intaking more Si atoms from the surrounding a-Si:H matrix, by forming an a-Si:H/In absorption interface in the front and a deposition SiNW/In interface at the rear. For simplicity and without losing generality, this liquid catalyst droplet can be approximated by a cuboid-bound box of w_c , l_c and h_c in length, width and height, respectively, as depicted in Fig. 2a, with a constant volume of $V \equiv l_c w_c h_c$. When such a catalyst droplet is advancing among a thin a-Si:H layer of h_a thick, the front *absorption* interface (the joining or touching region between a-Si:H layer and liquid catalyst droplet) can be approximated to be $S_{abs} = w_c \cdot h_a$, and thus the *influx* of Si atoms through this a-Si:H/In interface (or the rate of Si atoms entering from a-Si:H matrix into catalyst droplet) can be written as

$$J_{in} \sim v_{abs} \cdot S_{abs} \cdot \alpha / \Omega_{Si} = v_{abs} \cdot w_c \cdot h_a \cdot \alpha / \Omega_{Si}, \quad (1)$$

while the *deposition flux* of Si atoms (precipitation of Si atoms from the catalyst droplet to the SiNWs) at the rear SiNW/In interface, with a cross-section area of $S_{de} = w_c \cdot h_c$, as

$$J_{out} \sim v_{de} \cdot S_{de} \cdot h_c / \Omega_{Si} = v_{de} \cdot f \cdot w_c \cdot h_c / \Omega_{Si}, \quad (2)$$

where v_{abs} and v_{de} are the moving rates of the front absorption and the rear deposition interfaces, $f \equiv d_{SiNW}^2 / (w_c h_c)$ is the ratio of the cross section area of SiNW (of d_{SiNW} in diameter) over that of catalyst droplet, which can be considered as basically a constant $f \sim 0.16$ as the cross section dimension of the as-grown SiNW is more or less proportional to that of the catalyst droplet during a metal-droplet-assisted growth. $\alpha \sim 0.9$ is the volume contraction ratio of a-Si:H when being converted into c-SiNW and Ω_{Si} stands for the atomic volume of Si atoms, respectively. During a mass conservation growth, we should have $J_{in} = J_{out}$, while a balanced growth requires also in general $v_{abs} = v_{de}$. So, equalizing Eq.1 and Eq.2 leads to

$$w_c \cdot h_a \cdot \alpha = f \cdot w_c \cdot h_c \Rightarrow h_c = h_a \alpha / f \quad (3)$$

This represents more or less a criterion for achieving a balance lateral growth of SiNWs given a specific coating thickness of a-Si:H layer. It is also important to note that though post-growth SEM observation (for instance that in Fig. 2a) shows always a spherical droplet, it is not necessarily the case during the growth.

Under constant volume V_c constraints and growth balance requirement stated in Eq.3, the liquid catalyst droplet will try to minimize the overall surface/interface energies, hereafter defined as the surface Gibbs energy, which in the case of growth on a flat surface can be approximated as

$$G_{flat} = (w_c l_c + 2h_c l_c + 2h_c w_c) \sigma_c + w_c l_c \sigma_{in}. \quad (4)$$

Here, the first, the second and the third terms in the right-hand-side (rhs) bracket stand respectively for the catalyst liquid/vacuum interface areas on the top, the two sides (parallel to advancing direction) and the front and rear sides, where the interface/or surface energy of indium catalyst droplet is $\sigma_c = 0.5 \text{ N/m}$, as specified in Table 1. Meanwhile, the last term in the rhs of Eq. 4 represents the contribution arising from the bottom interface between the catalyst droplet and substrate, with an interface energy defined as the energy difference $\sigma_{in} \equiv \sigma_{In-SiN} - \sigma_{SiN}$ between the interface energy of indium/SiNx σ_{In-SiN} and the surface energy of the SiNx substrate σ_{SiN} , which has been estimated according to experimental observation of the contact angle of In droplet residing on a SiNx surface to be around $\sigma_{in} = \sigma_c \cos\theta$ (See Table 1 for adopted parameter values in the simulation).

Table 1 Summary of parameter values in simulation*

Quantities	Definition	Values (unit N/m)
σ_c	Indium/vacuum	0.5
σ_{SiN}	SiN sub/vacuum	-
	Indium/SiN sub	-
σ_{In-SiN}	$\sigma_{In-SiN} - \sigma_{SiN}$	$\sigma_c \cos(\theta)^{**}$
σ_{in}		

Notices:

* Only σ_c and σ_{in} enter in the modelling and simulation;

** $\theta \sim 65$ Degree is the contact angle measured experimentally between indium surface and outer substrate surface at triple-phase-line.

If we disregard the growth balance constraint written in Eq.3, minimizing the overall surface/interface Gibbs energy will lead to

$$G_{flat}^{min} = 3 \times 2^{\frac{2}{3}} (V \times \sigma_c)^{\frac{2}{3}} (\sigma_c + \sigma_{in})^{\frac{1}{3}} \quad (5)$$

with corresponding droplet width and height of $w_c = \left[\frac{2\sigma_c}{\sigma_c + \sigma_{in}} \right]^{\frac{1}{3}} V^{\frac{1}{3}}$ and $h_c = \left[\frac{(\sigma_c + \sigma_{in})^2}{4\sigma_c^2} \right]^{\frac{1}{3}} V^{\frac{1}{3}}$, respectively. In case $\sigma_c = \sigma_{in}$, the cuboid-bound box will recede into a cubic with $w_c = h_c = l_c = V^{\frac{1}{3}}$ that representing a sphere catalyst droplet. Now, imposing the growth balance constraint of Eq.3, the minimum Gibbs energy of an In catalyst droplet of volume V proceeding among an a-Si:H layer of h_a becomes

$$G_{flat}^{min-CS} = 4\sqrt{h_a V/f} \cdot \sigma_c + fV(\sigma_c + \sigma_{in}) \quad (6)$$

with corresponding dimensions of $w_c = \sqrt{Vf/\alpha h_a}$ and $h_c = h_a \alpha / f$. To reveal the consequence of imposing this growth balance constraint, we plot the extra Gibbs energy defined as $\delta G \equiv G_{flat}^{min-CS} - G_{flat}^{min}$ in Fig. 2b as a function of the size of the initial catalyst droplet $d_c \equiv V^{\frac{1}{3}}$ for a given a-Si:H layer thickness of $h_a = 25 \text{ nm}$. We see that the constraint Gibbs energy is always higher with $\delta G \geq 0$, except at a critical volume V_m ($d_m \equiv V_m^{\frac{1}{3}}$) where the catalyst droplet can proceed essentially without extra geometric deformation to satisfy the balance growth requirement in Eq.3.

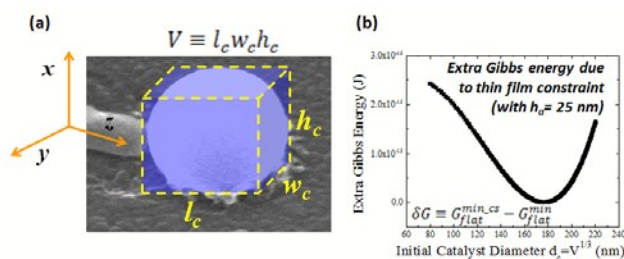


Fig. 2: (a) Enlarged SEM image of the catalyst droplet and in-plane SiNW, with schematic illustrations for the definition of the dimensions of the catalyst droplet in the formulation; (b) plots the extra Gibbs energy δG caused by the deformation of the liquid catalyst droplet, during the in-plane growth of SiNW, as a function of their initial catalyst droplet diameter $d_c \equiv V^{1/3}$.

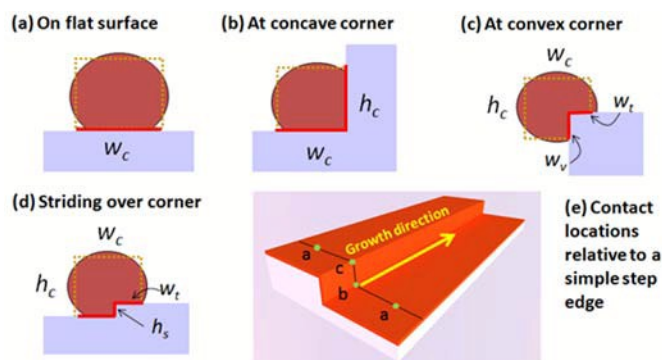


Fig. 3: (a)-(d) depict the 4 typical contact situations of a liquid catalyst droplet resting upon a flat, concave-corner, convex-corner and striding-over-corner local geometry, respectively, with corresponding positions (found around a step-edge) marked in (e).

When the catalyst droplets come to touch a simple step edge with a step height of h_s , the catalyst droplet forms an extra sidewall contact surface, which introduces thus an extra absorption frontier that will modify the mass conservation condition for the in-plane SiNW. In general, we consider here four contacting situations for the catalyst drop touching the step sites, as depicted in Fig. 3a to 3d and explained in more details below:

1) First, a planar contact between a catalyst droplet and a flat substrate surface, as seen in Fig. 3a. The overall Gibbs energy analysis of this situation has been derived above, see Eq.3, Eq.4 and Eq.6 for details.

2) Second, a concave (CC) contact between a catalyst droplet and the lower corner of a step, as depicted in Fig. 3b (with in general a negative local surface curvature, if we define the normal direction pointing outwards from the thin film material). In this situation, the overall Gibbs energy of the concave contact has been rewritten as

$$G_{cc} = (w_c + h_c)l_c(\sigma_c + \sigma_{in}) + 2w_ch_c\sigma_c \quad (7)$$

while the corresponding mass conservation equation/condition (see Fig. 3b), similar to that in Eq.3, is now formulated as

$$fw_ch_c = (w_c + h_c)h_a\alpha \quad (8)$$

Under this specific constraint condition, the minimum global Gibbs energy is

$$G_{cc}^{min} = \frac{Vf(ah_a - fh_c)(\sigma_c + \sigma_{in}) - 2\alpha^2 h_a^2 h_c^2 \sigma_c}{ah_a(ah_a - fh_c)} \quad (9)$$

3) Third, a convex (CV) contact between a catalyst droplet and a top edge of step (a situation that with a positive local curvature), as seen in Fig. 3c. For this situation, we have to define two absorption line lengths for the two contacting lines, indicated in Fig. 3c, on the vertical sidewall (w_v) and on the top of the step corner (w_t), respectively. Now, the sum of the overall surface Gibbs energy is written as

$$G_{cv} = (2w_c + 2h_c - w_t - w_v)l_c\sigma_c + (w_t + w_v)l_c\sigma_{in} + 2(w_ch_c - w_tw_v)\sigma_c \quad (10)$$

while the corresponding mass conservation condition is given as

$$f(w_ch_c - w_tw_v) = (w_v + w_t)h_a\alpha \quad (11)$$

Under this specific constraint condition, the minimum global Gibbs energy is

$$G_{cv}^{min} = \frac{2V\sigma_c}{h_c} + \frac{2\alpha h_a(w_t + w_v)\sigma_c}{f} + \frac{fV}{ah_a} \left((2h_c\sigma_c + 2w_tw_v\sigma_c/h_c)/(w_t + w_v) - (\sigma_c - \sigma_{in}) \right) \quad (12)$$

4) Last, for the situation of a large catalyst droplet, as shown in Fig. 3(d), which could grow along the step edge while striding over (SO) a step edge (contacting both the top and bottom surfaces) of h_s high, the global Gibbs energy becomes

$$G_{so} = (w_c + 2h_c - h_s)l_c\sigma_c + (w_c + h_s)l_c\sigma_{in} + 2(w_ch_c - w_th_s)\sigma_c \quad (13)$$

With the mass conservation condition written as

$$f(w_ch_c - w_th_s) = (w_c + h_s)h_a\alpha \quad (14)$$

and the minimum surface Gibbs energy of

$$G_{so}^{min} = \left(2\alpha^2 h_a^2 \sigma_c (h_c^2 h_s^2 + h_c(V - 2h_s^2(h_s + w_t)) + h_s(h_s(h_s + w_t)^2 - V)) + \alpha f h_a V (-4h_c^2 \sigma_c + h_c h_s (7\sigma_c - \sigma_{in}) + h_s(h_s(\sigma_{in} - 3\sigma_c) + w_s(\sigma_c + \sigma_{in}))) + f^2 V (h_c - h_s)(2h_c^2 \sigma_c + h_c h_s(\sigma_{in} - 3\sigma_c) + h_s \sigma_c (h_s - w_t) - h_s \sigma_{in} (h_s + w_t)) \right) / (\alpha h_a h_s (h_s + w - h_c)(\alpha h_a + f(h_s + h_c))) \quad (15)$$

For a typical a-Si:H coating layer thickness of $h_a = 15 \text{ nm}$, we plot in Fig. 4 the variations of minimum surface Gibbs energies G_{flat}^{min} , G_{cc}^{min} , G_{cv}^{min} and G_{so}^{min} , as a function of the initial catalyst size of d_c (with corresponding diameter of SiNWs displayed on the top frame). We found that, for smaller droplets with $d_c < 240 \text{ nm}$ (for in-plane SiNWs of $\sim 90 \text{ nm}$ in

diameter), the lowest Gibbs energy contact state is the flat surface (G_{flat}^{min}) or convex (G_{cv}^{min}) contacts. As a consequence, when a small catalyst droplet comes to contact the step-edge, it will be repelled away from the step-edge, instead of following the edge *track* to grow along. This is indeed a critical and new aspect that one has to take into account in designing the guiding step-edge height and a-Si:H coating thickness for thinner in-plane SiNWs. When the catalyst droplet becomes larger $d_c > 240 \text{ nm}$, the concave contact evolves as the state with the lowest Gibbs energy (G_{cc}^{min}) compared to others, as seen in Fig. 4. This implies that the running catalyst droplet will tend to stay at the root of the step-edge during the in-plane growth of SiNWs to form an extra absorption line on the vertical sidewall surface, and thus produce aligned SiNWs along the step-edge. This is the very basis for achieving an effective guided growth of the in-plane SiNWs. Furthermore, when the catalyst droplet becomes really large with respect to the step height, that is $d_c/2 \gg h_s$ (the division by a factor 2 arises from the consideration of the actual sidewall contact of a spherical droplet to the wall), the catalyst-edge contact scenario becomes a striding over (G_{so}^{min}) one as seen in Fig. 3d.

According to Gibbs energy plot in Fig. 4, when a large catalyst droplet comes to contact a relatively shallow step-edge, it is in general still energetically favourable compared to other situations. Thus, a guided growth can still be expected in this striding-over contact mode. However, as a matter of fact, if the catalyst droplet becomes larger and larger, the importance of such energy differentiation diminishes quickly, which means that it could simply *ignore* the shallow step there and go across it freely. We emphasize that this analysis has revealed a comprehensive picture of the detailed guiding growth mechanism of the in-plane SiNWs when interacting with a simple step-edge, which will enable us to delimitate clearly several parametric spaces where desired and stable guided growth could be sought. This framework could provide a practical guide to achieve or explain a precise position control of the in-plane SiNWs.

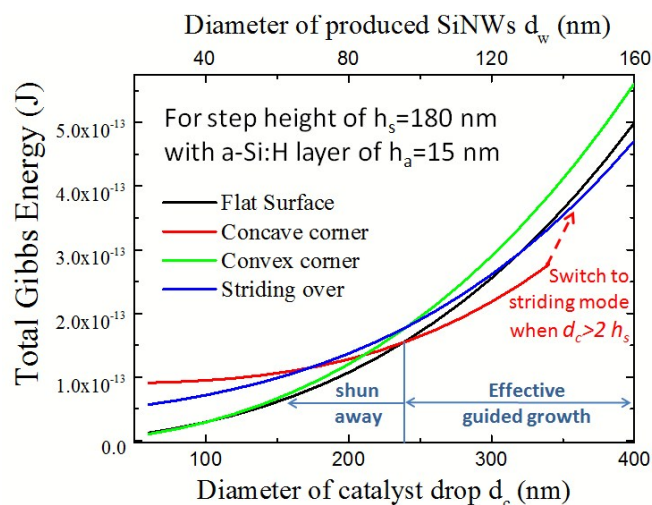


Fig. 4: Total surface Gibbs energy plots for the different contacting situations of a catalyst droplet as a function of their initial catalyst dimension (and the estimated diameters of the in-plane SiNWs).

Meanwhile, it is also important to note that, though the simulation presented in Fig. 4 has been carried out based a set of typical parameters of the step height h_s and a-Si:H coating thickness h_a , the model by itself is not limited by this specific parametric choice. Rather, in principle it represents a general modelling solution that will help to predict the guided growth behaviour with different combination of h_s and h_a inputs. Empirically, if one decreases (increases) the a-Si:H thickness h_a , the range of SiNW diameter for achieving a stable guided growth along the step-edge will shift towards thinner (thicker) ones. For example, in our previous work, the thinnest SiNW with obvious guided growth behaviour is found to be $<20\text{ nm}$ ²⁰.

We also testify these control principles against a series of direct experimental observations. As illustrated in Fig. 5a, a 180nm high SiNx step-edge has been prepared by reactive ion beam etching into a 300 nm thick SiNx layer deposited on Si wafer substrate, followed by an a-Si:H coating of $15 \pm 1.2\text{ nm}$ determined by ellipsometry measurement (not shown here).

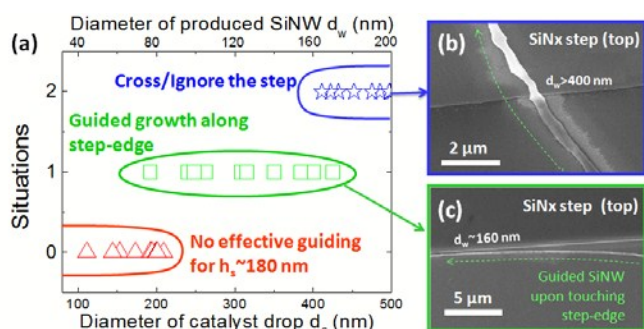


Fig. 5: (a) statistics of different observed interaction situations, with corresponding SEM images shown in (b)-(c), respectively.

Then, after the SiNWs growth procedure described above in the Experimental Section, we examine the different in-plane SiNWs that have interacted with step-edges in top view SEM observations, and record their final contacting situations as a function of the diameters of catalyst droplets and SiNWs. According to our statistics, the diameter of SiNW is more or less proportional to the size of catalyst droplet, roughly $\frac{d_{NW}}{d_c} \sim f^{\frac{1}{2}} \approx 0.4$, in Fig. 5a we provide both the diameters of the catalyst droplets (d_c) and the produced SiNWs, which are extracted and displayed as the bottom and top x -axis, respectively. Interesting enough, for the 32-sampled SiNWs, we found that the thinner SiNWs with $d_c < 180\text{ nm}$ (and $d_w < 70\text{ nm}$) usually go away from the guiding edge, instead of following the edge. In contrast, for thicker SiNWs produced by catalyst droplets with diameter between $200\text{ nm} < d_c < 400\text{ nm}$, the in-plane SiNWs were observed to grow along the guiding edge as seen for example the one shown in Fig. 5c. For even thicker SiNWs guided by large catalyst droplets with $d_c > 500\text{ nm}$, most of them simply continue their original directions and go across the step-edge, as witnessed in the SEM image in Fig. 5b. These experimental observations suggest that the interaction or guided growth dynamics can be indeed reasonably explained or predicted based on our analytic model established above. This also highlights the dominant role of the liquid catalyst droplet in in-situ tailoring or position the in-plane SiNWs.

More excitingly, we found that this step-edge guiding strategy can also be applied to accomplish more diversified SiNWs growth operations, not just being limited to guiding them along straight step-edge. For instance, we demonstrate in Fig. 6 a guided growth of single in-plane SiNW along a curve step line that introduces the SiNW from the left-bottom corner, grow through a series of turnings and release the in-plane SiNW into free space at a sharp edge turning (with an angle larger than 130 degree, as seen in the top-right inset of Fig. 6). While this SiNW-releasing dynamics has not yet been fully understood, we speculate that a sudden turning over the sharp edge tip will lead the catalyst droplet to go through a situation similar to that of a “convex-contact” (see Fig. 3c), which has been shown to be energetically unfavourable for large catalyst droplets (see the green line in Fig. 4). Therefore, continuous effective guiding of the catalyst droplet could be ruptured/or altered by this kinetic energy barrier to turn into flat space, as seen in the top-right inset of Fig. 6. Later on, after a free course of in-plane movement featuring somewhat random swaggering, the SiNW can be re-captured by another segment tip on the opposite side. Upon touching the guiding step-edge, the SiNW growth along the edge line faithfully. This observation implicates an interesting opportunity to accomplish a complete set of key in-situ growth control operations that include capturing, guiding and releasing of the in-plane SiNWs, and these abilities could indicate an effective and powerful means to position and deploy various nanowire-based functionalities in convenient planar substrate/architecture.

Moreover, it is also relevant to note that, though in this model discussed above, there is no consideration for the impact of specific growth orientation of the SiNWs, this however could be critical and important in directing in-plane SiNW through curved edge line or over sharp turning. This interesting aspect will be addressed in a more comprehensive model/or experimental investigations in our future works.

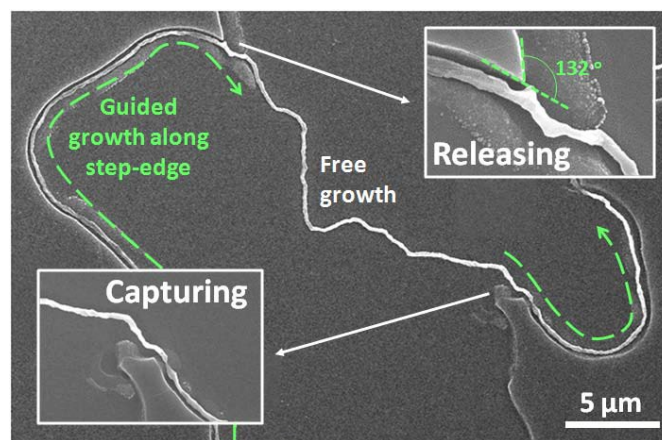


Fig. 6: SEM image of an in-plane SiNW guided by a curved step-edge. Enlarged views of the SiNW releasing at a sharp edge turning and re-capturing by another step edge segment are provided in the top-right and bottom-left insets, respectively.

Conclusion

In summary, we have developed an analytic model to describe the guiding growth dynamics of in-plane SiNWs, led by a catalyst droplet being constraint to substrate surface, via a

simple step-edge coated with a-Si:H thin film as solid precursor. We show that the variation of surface Gibbs energy of the catalyst droplets, under different contacting configuration, is the major driving force to lead the catalyst droplet into a pre-designed growth track. We demonstrate also a complete set of operations of the in-plane SiNWs with the aid of such a simple step-edge. These results provide a practical guide for employing this guiding growth strategy to achieve precise large area position control and even integration of the functional SiNWs channels.

Acknowledgements

The authors acknowledge the financial support from Jiangsu Province Natural Science Foundation (Young Talent Program No. BK20130573) and National Basic Research 973 Program under Grant Nos 2014CB921101, 2013CB932900, 2013CB632101, 2010CB934402 and NSFC under Nos 11274155 and 61204050.

Notes and references

^aSchool of Electronics Science and Engineering/Collaborative Innovation Center of Advanced Microstructures, Nanjing University, 210093, Nanjing, China

^bAddress Laboratoire de Physique des Interfaces et Couches Minces (LPICM), CNRS/Ecole Polytechnique (UMR 7642), Palaiseau, 91128, France.

^cCollege of Electronic Engineering and Electrical Automation, Chaohu University, 238000, Chaohu, China.

* Email: yulinwei@nju.edu.cn

- M. Mongillo, P. Spathis, G. Katsaros, P. Gentile and S. De Franceschi, *Nano Lett.*, 2012, **12**, 3074-3079.
- H. Yan, H. S. Choe, S. Nam, Y. Hu, S. Das, J. F. Klemic, J. C. Ellenbogen and C. M. Lieber, *Nature*, 2011, **470**, 240-244.
- R. Rurali, *Rev. Mod. Phys.*, 2010, **82**, 427.
- C. M. Lieber, *Mater. Res. Bull.*, 2003, **28**, 486-491.
- E. M. Freer, O. Grachev, X. Duan, S. Martin and D. P. Stumbo, *Nat. Nano*, 2010, **5**, 525-530.
- Y. Shan and S. J. Fonash, *ACS Nano*, 2008, **2**, 429-434.
- M. C. P. Wang and B. D. Gates, *Materials Today*, 2009, **12**, 34-43.
- D. Whang, S. Jin, Y. Wu and C. M. Lieber, *Nano Lett.*, 2003, **3**, 1255-1259.
- Y. Xiang, A. Keilbach, L. Moreno Codinachs, K. Nielsch, G. Abstreiter, A. Fontcuberta i Morral and T. Bein, *Nano Lett.*, 2010, **10**, 1341-1346.
- R. S. Wagner and W. C. Ellis, *Appl. Phys. Lett.*, 1964, **4**, 89.
- C. Y. Wen, M. C. Reuter, J. Tersoff, E. A. Stach and F. M. Ross, *Nano Lett.*, 2009.
- H. Wang, L. A. Zepeda-Ruiz, G. H. Gilmer and M. Upmanyu, *Nat Commun*, 2013, **4**.
- S. Misra, L. Yu, W. Chen and P. Roca i Cabarrocas, *The Journal of Physical Chemistry C*, 2013, **117**, 17786-17790.
- L. Yu, B. O'Donnell, P.-J. Alet, S. Conesa-Boj, F. Peiro, J. Arbiol and P. Roca i Cabarrocas, *Nanotechnology*, 2009, **20**, 225604.
- J. F. Dayen, A. Romyantseva, C. Ciornei, T. L. Wade, J. E. Wegrowe, D. Pribat and C. S. Cojocaru, *Appl. Phys. Lett.*, 2007, **90**, 173110.
- S. A. Fortuna, J. Wen, I. S. Chun and X. Li, *Nano Lett.*, 2008, **8**, 4421-4427.
- C. Zhang, X. Miao, P. K. Mohseni, W. Choi and X. Li, *Nano Lett.*, 2014.
- C. Martin, *Nat. Mater*, 2012, **11**, 8.
- L. Yu, P.-J. Alet, G. Picardi and P. Roca i Cabarrocas, *Phys. Rev. Lett.*, 2009, **102**, 125501.
- L. Yu, W. Chen, B. O'Donnell, G. Patriarche, S. Bouchoule, P. Pareige, R. Rogel, A. C. Salaun, L. Pichon and P. Roca i Cabarrocas, *Appl. Phys. Lett.*, 2011, **99**, 203104-203103.
- L. Yu and P. Roca i Cabarrocas, *Phys. Rev. B*, 2009, **80**, 085313-085315.
- L. Yu and P. Roca i Cabarrocas, *Phys. Rev. B*, 2010, **81**, 085323.
- W. Chen, L. Yu, S. Misra, Z. Fan, P. Pareige, G. Patriarche, S. Bouchoule and P. R. i. Cabarrocas, *Nat Commun*, 2014, **5**, 4134.
- L. Yu, M. Oudwan, O. Moustapha, F. Franck and P. Roca i Cabarrocas, *Appl. Phys. Lett.*, 2009, **95**, 113106.
- L. Yu and P. Roca i Cabarrocas, *PHYSICA E*, 2012, **44**, 1045-1049.